Available online at www.sciencedirect.com
ScienceDirect
Journal of Hazardous Materials 140 (2007) 488–503
Journal of Hazardous Materials
www.elsevier.com/locate/jhazmat

An LNG release, transport, and fate model system for marine spills

Malcolm L. Spaulding [a,b,*], J. Craig Swanson [a], Kathy Jayko [a], Nicole Whittier [a]

[a] *Applied Science Associates, Inc., 70 Dean Knauss Drive, Narragansett, RI 02882, United States*
[b] *Ocean Engineering, University of Rhode Island, Narragansett, RI 02882, United States*

Available online 21 October 2006

Abstract

LNGMAP, a fully integrated, geographic information based modular system, has been developed to predict the fate and transport of marine spills of LNG. The model is organized as a discrete set of linked algorithms that represent the processes (time dependent release rate, spreading, transport on the water surface, evaporation from the water surface, transport and dispersion in the atmosphere, and, if ignited, burning and associated radiated heat fields) affecting LNG once it is released into the environment. A particle-based approach is employed in which discrete masses of LNG released from the source are modeled as individual masses of LNG or spillets. The model is designed to predict the gas mass balance as a function of time and to display the spatial and temporal evolution of the gas (and radiated energy field).

LNGMAP has been validated by comparisons to predictions of models developed by ABS Consulting and Sandia for time dependent point releases from a draining tank, with and without burning. Simulations were in excellent agreement with those performed by ABS Consulting and consistent with Sandia's steady state results.

To illustrate the model predictive capability for realistic emergency scenarios, simulations were performed for a tanker entering Block Island Sound. Three hypothetical cases were studied: the first assumes the vessel continues on course after the spill starts, the second that the vessel stops as soon as practical after the release begins (3 min), and the third that the vessel grounds at the closest site practical. The model shows that the areas of the surface pool and the incident thermal radiation field (with burning) are minimized and dispersed vapor cloud area (without burning) maximized if the vessel continues on course. For this case the surface pool area, with burning, is substantially smaller than for the without burning case because of the higher mass loss rate from the surface pool due to burning. Since the vessel speed substantially exceeds the spill spreading rate, both the thermal radiation fields and surface pool trail the vessel. The relative directions and speeds of the wind and vessel movement govern the orientation of the dispersed plume.

If the vessel stops, the areas of the surface pool and incident radiation field (with burning) are maximized and the dispersed cloud area (without burning) minimized. The longer the delay in stopping the vessel, the smaller the peak values are for the pool area and the size of the thermal radiation field. Once the vessel stops, the spill pool is adjacent to the vessel and moving down current. The thermal radiation field is oriented similarly. These results may be particularly useful in contingency planning for underway vessels.

1. Introduction

Liquefied natural gas (LNG) has been transported by sea, using specially designed ships, since 1959. These vessels have an excellent safety record and provide a critical link in transporting LNG from production facilities to customer locations. According to Sandia [1] the combination of higher natural gas prices, rising demand for natural gas, and lower LNG production costs are setting the stage for a dramatic increase in LNG trade. Estimates are that the world-wide trade will increase by 35% by 2010. US imports are projected to double over the next decade. The US currently has six LNG re-gasification terminals (Lake Charles, LA; Everett, MA; Elba Island, GA; Cove Point, MD; offshore in the Gulf of Mexico; Penuelas, PR) in operation. More than 50 new terminal sites are under consideration in the US Marine terminals are often being proposed near major consumer markets, and hence near major population centers, to minimize distribution costs, although a number are located offshore.

Systematic safety standards and protocols exist for analysis of risk of LNG spills or releases from storage terminals and facilities on land. There are no equivalent standards or guidelines for the evaluation of safety or the consequence of LNG spills in marine waters [1]. As a first step in addressing this issue ABS Consulting [2], under contract to the Federal Energy Regulatory Commission (FERC), and Sandia Laboratory [1],

* Corresponding author at: Ocean Engineering, University of Rhode Island, Narragansett, RI 02882, United States. Tel.: +1 401 874 6666; fax: +1 401 874 6837.
E-mail address: spaulding@oce.uri.edu (M.L. Spaulding).

0304-3894/$ – see front matter © 2006 Elsevier B.V. All rights reserved.
doi:10.1016/j.jhazmat.2006.10.049

under contract to the US Department of Energy (DOE), independently reviewed the consequence assessment methodologies that are available to model releases of LNG spills on water. Both concentrated on four papers or reports (Fay [3], Lehr [4], Quest [5], and Vallejo [6]) that provide models for key processes in the transport and fate of LNG released on the sea surface. Both studies found that none of the existing models provided a comprehensive tool to assess the consequences of LNG spills. Based on review of the reports, the principal limitations are that none of the four models: (1) included all the key transport and fate processes; (2) had been thoroughly validated; (3) could be used to perform stochastic simulations of releases; (4) displayed linkage to environmental forcing data (currents, waves, and winds); (5) addressed the breakup of the LNG spill once it was released; (6) provided consistent information on the LNG mass balance or location of the LNG in space and time or (7) provided a user friendly graphics-based interface.

Based on an in-depth review of the literature, ABS Consulting [2] recommended particular algorithms that should be used for each of the key transport and fate processes. These algorithms were typically based on a combination of theoretical formulations and empirical relationships derived from laboratory and field observations. Sandia [1], on the other hand, recommended the use of a suite of computational fluid dynamics (CFD) codes for predicting spreading, dispersion in the atmosphere, and fire. Because of the high computational costs associated with Sandia's CFD based approach, its application will, of necessity, be restricted to studying only a select number of very high consequence events at a particular site. These sites are likely to include complicated topography and the presence of buildings and infrastructure. The goal of the present work was to develop a state of the art, integrated model system to predict the release, transport, fate (evaporation, dispersion, and burning) and impact of LNG spills in marine waters. An algorithm-based modeling strategy that relies on the best understanding of the key transport and fate processes was used. This is the strategy recommended by ABS Consulting [2] and the approach used in the four model systems they reviewed. The present effort focuses on developing: (1) a fully integrated, modular systems approach, including gas and fire dynamics, with appropriate feedback mechanisms, (2) the ability to model time dependent, stationary or moving, releases with variable environmental forcing (winds and currents), (3) a comprehensive suite of model outputs, in accordance with regulatory requirements and impact assessment procedures, (4) the ability to perform both deterministic and eventually stochastic (risk assessment) simulations, (5) a fully integrated geographic system (GIS) to allow visualization of infrastructure and supporting data, (6) visualization tools to animate model predictions for pool spreading, vapor dispersion, and fire, and (7) the ability to link to rapidly evolving coastal ocean observing and forecasting systems (point observations, satellite data, high frequency radar systems, drifting buoys, hydrodynamic/meteorological models with various grid systems).

Section 2 begins with an overview of the modeling strategy and then summarizes model input, the suite of algorithms implemented, and model output. Section 3 presents a comparison of the predictions of the present model with test cases presented in ABS Consulting [2] and Sandia [1] and serves to validate the particle-based approach employed here. This validation is used to ensure that the model gives results in agreement with prior implementation of the algorithms but does not represent an independent verification of model predictions against observations. Application of the model to time dependent stationary and moving releases is presented in Section 4, conclusions in Section 5.

2. Model development strategy

2.1. Overview

LNGMAP is organized as a discrete set of linked algorithms that represent the fate and transport processes affecting LNG once it is released into the environment. At present, the system models the release rate, spreading, transport on the water surface, evaporation from the water surface, transport in the atmosphere, and, if ignited, burning and the associated radiated heat field. The model does not currently include rapid phase transition or dissolution into the water column. The latter maybe important in assessing the biological impacts of releases from sub-sea sources (e.g., pipelines). The model is designed to predict the LNG mass balance as a function of time in both liquid and gaseous states and to display the spatial and temporal evolution of the gas (and radiated energy field).

To allow a consistent method to track both the liquid and gaseous states of LNG for time dependent releases, a particle-based approach is employed. This strategy is widely used in oil and chemical spill models for the marine environment (for examples see ASA [7,8]). In this approach discrete masses of LNG, termed spillets, are modeled individually. The mass balance and position of each independent spillet are tracked over time. In practice, surface spillets are generated as LNG is released from the source, with the number and size dependent on the release rate and time step. These are tracked on the water surface until all the surface mass has disappeared. The spillets will naturally separate from each other on the sea surface due to the transport by surface currents and the differential release times. Atmospheric spillets are generated as a result of evaporation from a surface spillet, with the number and size dependent on the number of surface spillets and evaporation rate, respectively. Atmospheric spillets are tracked until all the gas is consumed by burning or dispersed outside the study area. Summation of the amount of LNG over all surface (liquid) and atmospheric (gas) spillets provides the mass of LNG in each environmental compartment as a function of time. The location of the spillets provides information on the spatial distribution of the LNG with time.

In order to maintain a computationally reasonable number of spillets, aggregation is used to reduce the number of spillets. Spillets are always combined into a single larger spillet if their edges touch. The user can specify more stringent aggregation rules; for example, requiring that two spillets overlap by more than 50% before they can be combined into one larger spillet. A sensitivity study investigated the effect of the model time step on predicted areas. Time steps ranging from 0.01 to 0.2 s were

considered. The predicted LNG surface pool area and (in the case of burning) area affected by thermal intensity (for a given intensity interval) were found to be relatively insensitive to time step. Given the small spatial scales (100 s m to several km) and temporal scales (seconds to minutes) of interest in LNG spill modeling, care has been taken to develop gridding strategies and output time intervals that allow accurate visualization of the LNG spill.

Features proposed for the present application include: a full suite of fate and transport algorithms (including burning); global application; PC based; fully integrated GIS; real time access to national/international data bases for surface winds, currents, and waves; robust, widely used and tested graphics user interface; options for simulation of individual events or stochastic based (not currently implemented) predictions; mass balance summary; animation of spatial/temporal mass distribution in environmental compartments; outputs that link to established response and impact metrics; spatial scales (100 s m to 5 km) and temporal scales (seconds to minutes) typical of LNG releases; and readily extensible to assess human and environmental (biological) impacts.

2.2. Model input, algorithms and outputs

Model input, algorithms, and output are briefly summarized below. As currently implemented the model is run in a deterministic (discrete simulation of one event) mode.

2.3. Model input

Model inputs are kept to a minimum to simplify the specification of a scenario. The physical and chemical characteristics of LNG and associated rate parameters required for the model are stored in a database to facilitate data organization and updating. Only a few parameters are required to define the LNG release and environmental conditions. These include:

- The release is specified as one of the following:
  - A constant release rate (user specifies rate and duration of release).
  - A time dependent release rate controlled by the tank characteristics, initial depth of fluid in tank, size of tank rupture, and discharge coefficient. The rupture is assumed to be at the water surface.
- The spill location. The location may be stationary or moving. If moving, the vessel's path and speed are required.
- Surface currents, wind speed/direction, sea surface/air temperature, and relative humidity. (The impact of waves on surface transport is approximated through a wind/wave induced drift algorithm that is based on wind speed and direction, see discussion below.)

2.4. Model algorithms

Presented below is a summary of the algorithms used for each model transport and fate process. References are provided as appropriate for each algorithm. Algorithm selection follows the recommendation in the ABS Consulting [2] model evaluation report and FERC's staff response to report comments [9], unless otherwise noted. There has been no attempt to validate these algorithms, neither to compare these algorithms with others that represent the process nor to defend their selection beyond noting that they were recommended by ABS Consulting. Other algorithms could have been as readily employed.

2.5. Transport on sea surface

The transport of LNG on the sea surface is based on a Lagrangian particle formulation, with each spillet modeled as an independent entity. This strategy is widely used in oil and chemical spill modeling [7,8]. The advective transport of a spillet is modeled using the simple evolution

$$\mathbf{X}_{i+1} = \mathbf{X}_i + \Delta t\, \mathbf{U}_i \tag{1}$$

where $\mathbf{X}_{i+1}$ and $\mathbf{X}_i$ are the horizontal position vectors for the spillet at locations $i+1$ and i, respectively. Δt the model time increment, and $\mathbf{U}_i$ is the surface current velocity vector at location i. Since the time steps for LNG simulations are small (seconds) and the environmental forcing varies slowly over the short simulation times, this simple, first order advective scheme is adequate. $\mathbf{U}_i$ in Eq. (1) typically includes currents (transport) due to waves, winds, tides, and residual flows. Estimates of these currents can be obtained from observations, model predictions, or some combination of the two. It is characteristic in spill models to represent the wind and wave induced transport in terms of a drift factor and angle. The drift factor, typically in the range of 2–3.5%, is multiplied by the 10 m wind speeds to estimate the wind induced surface current speed. The drift angle, θ, is the direction of the wind and wave induced surface currents, relative to the wind direction (to the right of the wind in the northern hemisphere). Values of θ typically vary from 0° to 20°. In addition the LNG spillets are dispersed horizontally at the sea surface due to turbulence generated by the wind, waves, or shear in the current field. Dispersive transport is modeled as a first order Markov process (random walk model) [10] and hence represents a solution to the two-dimensional convective diffusion equation. In practice several hundred spillets are required to accurately represent the dispersive transport.

2.6. Release rate from vessel/container

A review by ABS Consulting [2] of available models found none that directly incorporate the physical characteristics of an LNG tank and the double hull construction of LNG tankers. A simple orifice model driven by gravity is therefore used, with the understanding that it will likely overestimate the release rate since it assumes a single wall tank with a free surface at atmospheric pressure, and no interaction with the ship's structure. The implementation of the orifice model in LNGMAP presently assumes the tank breach is at water level.

The standard equation that represents discharge through an orifice is:

$$Q = C_\mathrm{d} A\, (2\, g H)^{1/2} \tag{2}$$

where Q is the discharge from the orifice (m^3/s), C_d the discharge coefficient (typically 0.65), A the area of the orifice (m^2), g the gravitational acceleration (m/s^2), and H is the head on the orifice, measured from the center of the orifice to the free surface (m).

LNGMAP presently assumes the tank has a constant cross-sectional area. This results in a linearly decreasing release rate with time. At each time step (typically a fraction of a second) over the duration of the release, the calculated mass of LNG released is used to create a surface "spillet" of LNG. The movement of each spillet is tracked individually.

2.6.1. Spreading on water surface

An analysis of various spreading algorithms by ABS Consulting [2] concluded that friction effects can be important in LNG pool spreading, particularly for large, short-term releases. Therefore, spreading is calculated following the approach used in the GASP (gas accumulation over spreading pools) model of Webber [11], as described in TNO [12]. The "shallow layer equations" describe the spreading phenomena in terms of a balance of inertia, gravity, and friction forces. In cylindrical form, the conservation of momentum equation takes the form:

$$\frac{d^2r}{dt^2} = \frac{4\Phi g_r h}{r} - C_F \tag{3}$$

where d^2r/dt^2 is the inertia term, $4\Phi g_r h/r$ the gravity term, Φ the coefficient, a function of a dimensionless shape factor that describes the LNG pool thickness profile, g_r the reduced gravitational acceleration ($=g(\rho_w - \rho_{LNG})/\rho_w$), h the pool thickness (m), r the pool radius (m), C_F the turbulent or viscous resistance term (friction), and ρ_w, ρ_{LNG} is the density of water and LNG, respectively (kg/m^3).

A new spillet is released every time step, and spreads radially at a rate consistent with its physical characteristics. Spillets that overlap (by a fraction specified by the user) are combined into a single spillet with an increased radius to account for the additional mass. The effect of a moving release source or strong environmental forcing is to spread the spillets apart, resulting in a spatially dispersed footprint, typically an elongated plume. In the limiting case of a stationary source with negligible environmental forcing, a single circular pool represents the spilled LNG.

2.6.2. Evaporation

In the case where LNG vapor is not ignited over the pool, vaporization is controlled by the rate of heat transfer from the water to the LNG.

$$H_V = k_H(T_w - T_b) \tag{4}$$

where H_V is the heat flux ($J/(m^2\,s)$), k_H the film-boiling heat transfer coefficient ($J/(m^2\,s\,K)$), T_w the water temperature (K), and T_b is the LNG boiling point (K).

The film boiling heat transfer coefficient is calculated using the model/correlation of Kilmenko [13]. Assuming the water beneath the spill remains well mixed and at its initial temperature, the value of k_H remains constant, and hence the heat flux (H_V) is constant. The rate at which mass is evaporated from the circular pool is

$$m_e = \frac{\pi r^2 H_V}{h_v} \tag{5}$$

where m_e is the mass evaporation rate (kg/s), and h_v is the heat of vaporization (J/kg).

As mass is evaporated from each spillet, it is removed from the surface pool (resulting in less volume on the surface and a contracting pool size) and placed in the atmosphere.

2.7. Dense gas vapor dispersion

LNGMAP currently uses a simple random walk technique to simulate the three dimensional transport and turbulent dispersion of the LNG that evaporates. At each time step particles (atmospheric spillets) are created to represent the mass evaporated from each surface spillet. Atmospheric spillets are transported in response to wind forcing and dispersed due to horizontal and vertical turbulence. The turbulent dispersion coefficients are based on the Pasquill–Turner stability class [14,15,10]. To simulate the dense gas nature of cold vapor, particles are assigned a very small vertical dispersion coefficient until they are assumed to warm sufficiently for the gas to become buoyant. The time needed to warm was determined by running numerous DEGADIS [16] simulations under different meteorological conditions. Warming times are typically on the order of 15–20 s for the simulations presented here. Output shows the spatial and temporal variation in the vapor plume, and the extent of the plume within the flammability limits (5–15% LNG by volume).

2.8. Burning rate and thermal radiation from pool fire

In the case of fire, vaporization is controlled by heat transfer from both the water and the fire to the LNG. A constant burning rate that accounts for the contributions of both water and fire is used. The rate at which mass is removed from the pool due to burning is

$$m_b = \pi r^2 b \tag{6}$$

where m_b is the mass removal rate (kg/s), and b is the burning rate ($kg/(m^2\,s)$).

Note that even though the burning rate per unit area is constant in Eq. (6), the mass removal rate from burning is dynamically linked to the spill spreading rate through the spill radius.

To determine the thermal radiation emitted by the burning LNG, a solid flame model describes the pool fire with the flame described as a tilted circular cylinder. The flame height in the presence or absence of winds is determined using the correlations of Thomas [17]. The flame tilt angle is determined using the method of Rew and Hulbert [18]. The pool fire height and diameter are used to calculate the view factor as defined in TNO [12]. Finally, the thermal radiation intensity, i, at a location outside the flame envelope is determined following Mudan [19] by

$$i = EF_{12}\tau \tag{7}$$

where E is the average emissive power at the flame surface (kW/m^2), F_{12} the vectoral sum of the horizontal and vertical target configuration view factors, and τ is the atmospheric transmissivity.

The thermal radiation generated by each spillet's pool fire or flamelet is summed to generate a map of the total thermal intensity.

The model is incremented in time, at finite time intervals or time steps, to represent time dependent releases and the resulting impact of fate and transport processes. The following sequence of calculations is performed at each time step (and for each spillet) and then repeated to increment the solution in time. Calculation sequences are provided for both the surface and atmospheric spillets:

2.8.1. For the water

(1) Determine the amount of LNG released from the vessel, include this mass in a spillet.
(2) Use the spreading algorithm to determine the spillet radius.
(3) Determine the mass of LNG lost to the atmosphere by evaporation or burning.
(4) Remove the amount of LNG mass evaporated or burned from the spillet.
(5) Reduce the number of spillets by aggregation (combine spillets that overlap by more than a fixed percentage).
(6) Advect and disperse surface spillets using a two dimensional random walk model.

2.8.2. For the atmosphere

(1) Create atmospheric spillets for each mass of LNG lost from each surface spillet by evaporation.
(2) Advect and disperse atmospheric spillets using three dimensional random walk model.

2.8.3. Model output

The results of a simulation can be displayed in several ways, including:

- Temporal evolution (animations) of spatial distributions (2D) of LNG on the sea surface and in the atmosphere over the simulation period. Given the discrete particle nature of the model, contour maps for liquid gas on the sea surface or gas dispersed into the atmosphere are generated by overlaying a grid system covering the extent of the particle dispersion and interpolating the individual particle masses onto the grid system.
- Time dependent mass balance of LNG for both liquid and gaseous states in various environmental compartments (source, sea surface, atmosphere/burned).
- Time dependent contours of LNG vapor concentration values in the atmosphere with time, highlighting the lower flammability limit (LFL) (5% concentration), upper flammability limit (UFL) (15% concentration), and human effects thresholds.
- Time dependent contours of radiated heat flux in the event of fire, highlighting contours of 38, 25, 12, and 5 kW/m^2 (spanning the range of damage to equipment, ignition of wood structures, melting of plastic and fatalities, and causing skin burns).
- Thermal radiation time history at user-selected locations. Impact on individuals, structures, materials and facilities is best assessed in terms of thermal dose received (thermal radiation level integrated over time).

3. Validation of model system

To validate the particle-based implementation of the individual process algorithms given in Section 3, simulations were performed for case examples presented in the ABS Consulting ([2]; Appendices C and D) and Sandia [1] reports. Ideally model validation would use experimental or actual spill data but no data sets exist for large spill events. This validation exercise serves to show that the present implementation of a particle based strategy gives results that are the same or consistent with more conventional semi-analytic techniques.

An LNG release via a tank rupture was modeled using the orifice release parameters presented by ABS Consulting [2]. A release of 12,500 m^3 of LNG through a 1 m diameter hole with an initial fluid height of 13 m above the release point was calculated. The discharge coefficient was set to 1.0, and the model time step was set at 0.1 s. The release continues until the fluid level in the tank had dropped to the hole height. ABS Consulting calculated an initial release rate of 5300 kg/s, linearly decreasing to 0.0 over a period of 33.3 min. The present calculations yielded exactly the same results.

3.1. With burning

Figs. 1–3 show a comparison between the ABS Consulting [2] and present model predicted evaporation rate, pool radius, and thermal incident radiation flux (at 300, 500, and 1000 m from the source) versus time, for the case with burning. The pool radius and evaporation rate increase rapidly with time (0–200 s) as the LNG spreads on the water surface. Once the tank discharge rate

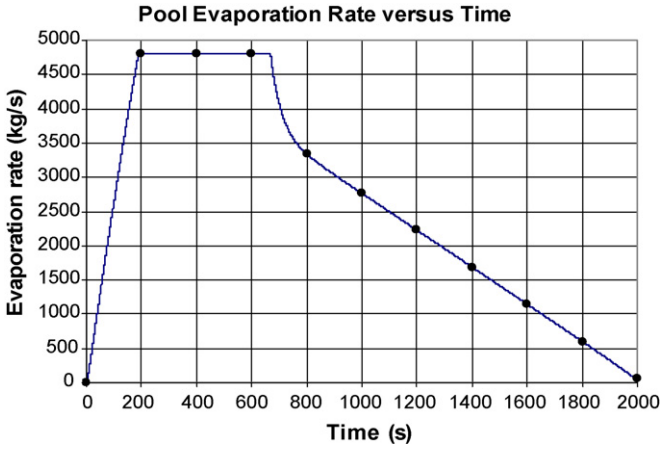

Fig. 1. Comparison of LNGMAP (solid line) and ABS Consulting [2] (circle) estimates for evaporation rate (kg/s) vs. time (s) for a 12,500 m^3 release from a 1 m diameter hole, with burning.

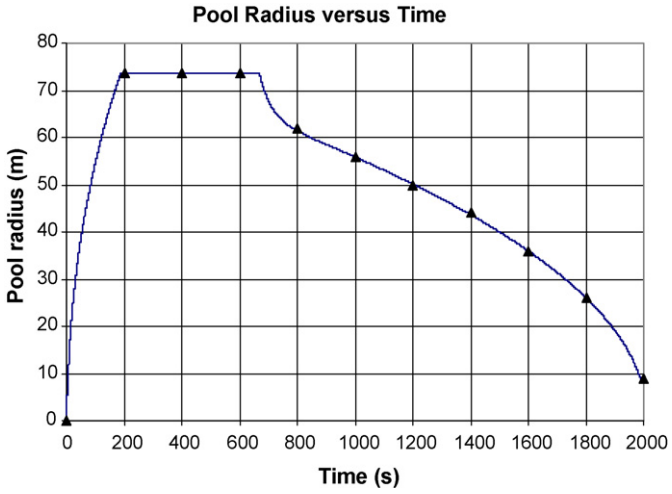

Fig. 2. Comparison of LNGMAP (solid line) and ABS Consulting [2] (triangle) estimates for pool radius (m) vs. time (s), for a 12,500 m^3 release from a 1 m diameter hole, with burning.

is in balance with the evaporation rate the pool radius becomes fixed (200–650 s). After this point the pool radius and evaporation rate decrease rapidly until the pool disappears several minutes after the release stops. During the initial portion of this phase (650–800 s) the evaporative losses exceed the release rate and the pool size decreases rapidly. After about 800 s, from the start of the release, the evaporative losses from the pool are in balance with the declining rate of release as the tank empties. The time dependency of the thermal radiation contours mirrors the pool evaporation rate. The present model captures the time dependency of each variable and is in excellent agreement with the ABS Consulting predictions.

3.2. Without burning

Simulations were next performed for the above scenario, but assuming that burning did not occur. The release rate for this case is the same as for the "with burning" case. Figs. 4 and 5 show a comparison between the ABS Consulting and present model

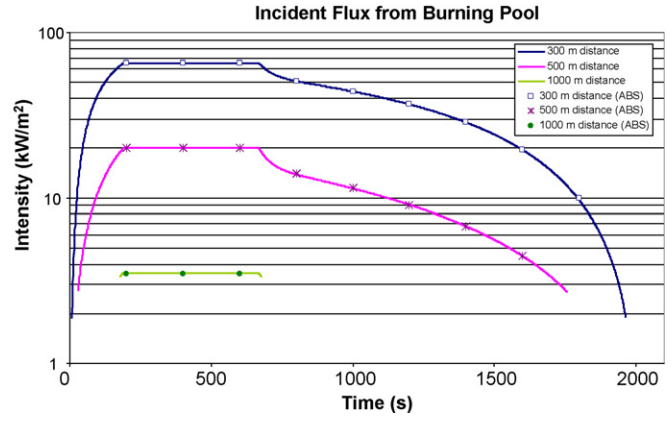

Fig. 3. Comparison of LNGMAP (solid line) and ABS Consulting [2] (symbols) estimates for incident thermal radiation intensity (kW/m^2) vs. time (s), for a 12,500 m^3 release from a 1 m diameter hole at 300, 500, and 1000 m from the source, with burning.

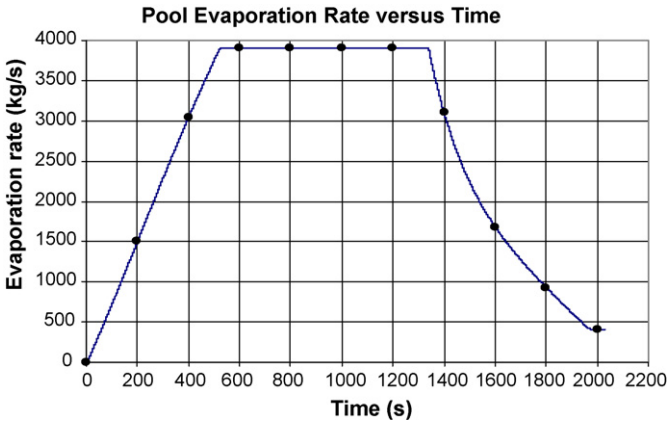

Fig. 4. Comparison of LNGMAP (solid line) and ABS Consulting [2] (triangles) estimates for evaporation rate (kg/s) vs. time (s), for a 12,500 m^3 release from a 1 m diameter hole, without burning.

predicted evaporation rate and pool radius versus time, respectively. Once again the agreement between the present model and ABS Consulting is excellent.

Comparing Fig. 1 (with burning) and (without burning) shows that the evaporative rate versus time curves are similar in shape. The burning case (Fig. 1) has a faster rise (200 s) to the maximum rate, a higher and longer duration at the maximum rate, and a more rapid and shorter duration decline at the end of the release. The pool radius versus time, with (Fig. 2) and without (Fig. 5) burning cases, is also similar in shape. The maximum pool radius is smaller and its duration is shorter for the burning case. The rate of increase (decrease) in pool diameter is faster early (late) in the tank emptying time for the burning case. With burning the evaporative loss rate is enhanced relative to the no burning case. Since more mass is removed from the surface due to burning the pool radius and duration at maximum radius, with burning, is correspondingly smaller than for the no burn case. The present model captures these dynamics.

The excellent agreement noted above is of course not surprising since LNGMAP implements the algorithms recommended in the ABS Consulting report. The results do show however that the particle-based implementation is consistent with ABS Consulting's results.

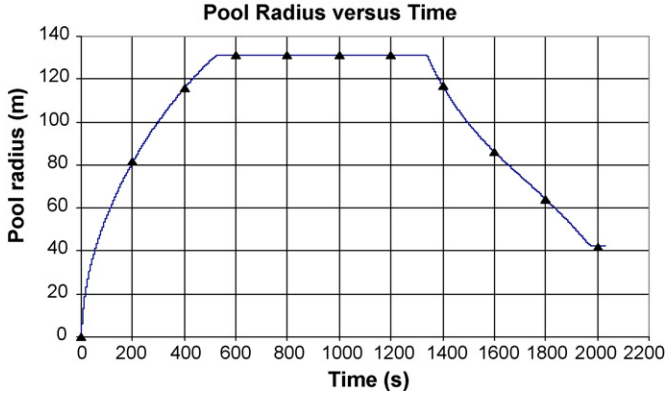

Fig. 5. Comparison of LNGMAP (solid line) and ABS Consulting [2] (triangles) estimates for pool radius (m) vs. time (s), for a 12,500 m^3 release from a 1 m diameter hole, without burning.

Table 1
Comparison of Sandia [1] and LNGMAP predictions for three hole sizes

	Hole size = 1 m^2		Hole size = 2 m^2		Hole size = 5 m^2	
	Sandia	LNGMAP	Sandia	LNGMAP	Sandia	LNGMAP
Pool diameter (m)	148	194	209	246	330	282
Spill duration (min)	40	40.5	20	20.2	8.1	8.1
Burn time (min)	–	40.7	–	20.6	–	13.6
Distance to 37.5 kW/m^2 (m)	177	206	250	311	391	316
Distance to 5 kW/m^2 (m)	554	622	784	731	1305	948

Sandia [1] reported the results of simulations with release holes of 1, 2, and 5 m^2, a total release of 12,500 m^3 with an initial tank level of 15 m above the breach. They provide predictions of the pool diameter (m), spill duration (min), and distance (m) to 37.5 and 5 kW/m^2 thermal radiation incident fluxes, with burning. LNGMAP simulations were performed for each case attempting to match each input parameter based on data given in the Sandia report. Some notes of caution prior to presenting the results include:

- Sandia did not provide information on the tank cross sectional area. The present study estimated this based on volume spilled and liquid level in the tank.
- The heat flux, from the water and fire to the LNG pool, were not specified in the Sandia report.
- Sandia used an average flow rate over the discharge period and hence the pool diameter and distances to various thermal radiation contours are based on averages. The present results are time dependent and report the maximum values for each case. Sandia used a very simple mass balance approach to spreading while the present study used a more sophisticated dynamics based approach.
- Sandia used a different correlation to determine flame height than was used by the ABS Consulting [2] study and the present study.

Comparison of the present simulations with those report by Sandia are provided in Table 1. LNGMAP results are in excellent agreement with Sandia for the spill duration, with the release time scaling inversely with the hole diameter. LNGMAP predictions for pool diameter and the distances to the two thermal radiation contours are approximately 10–20% larger than the Sandia values for the 1 and 2 m^2 hole sizes and 10–38% lower for the largest hole size. These differences can be attributed to differences between the time dependent LNGMAP discharge calculations and the Sandia steady state approximation, and LNGMAP's more sophisticated spreading model.

4. Application to selected cases with moving and stationary sources

To illustrate some of the key features of LNGMAP related to its ability to handle a time varying release from both a sta-

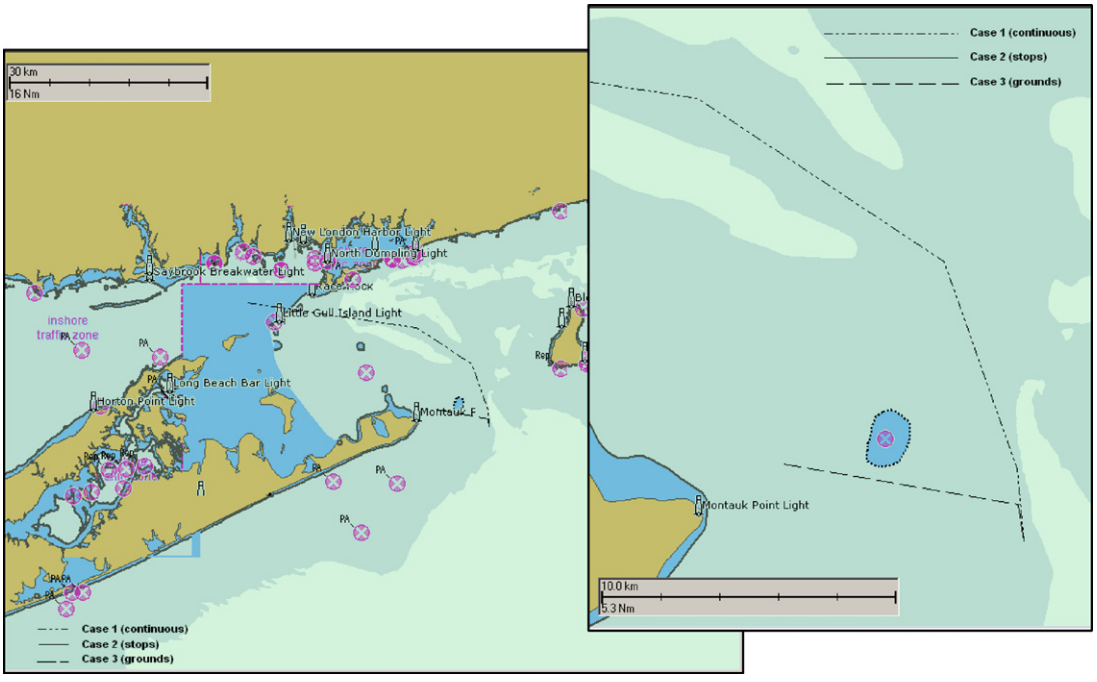

Fig. 6. Block Island sound study area showing the path/location of the LNG tanker if the vessel continues on course (Case 1), if it stops (Case 2), and if diverts its path to intentionally ground (Case 3).

tionary and moving source and to incorporate environmental forcing, simulations of three *hypothetical* scenarios for a vessel entering Block Island Sound, in the vicinity of Montauk Point, and headed toward Long Island Sound (Fig. 6) were performed. These hypothetical scenarios are unrelated to any proposed LNG terminals in southern New England. The scenarios included the LNG tanker: (1) proceeding on its planned course traveling at 7.5 m/s (15 kt) (Case 1—on course), (2) immediately stopping (within 3 min) and anchoring (Case 2—stopping), and (3) changing direction headed toward the closest location to ground the vessel (Case 3—grounding). In all cases the hole size is 1 m in diameter. The simulation time step was 0.1 s. The winds are assumed constant from the southwest at 5 m/s and the Pasquill stability category was moderately unstable (Class B), typical of summer conditions. Tidal currents are provided by a hydrodynamic model of the study area and vary both spatially and temporally [20]. The total volume spilled in each case is 12,500 m^3, with an initial tank head of 13 m above the release point. The release is complete over a period of 33.3 min. Two series of simulations were performed assuming: (1) the LNG on the sea surface ignited immediately and burned completely and (2) the LNG evaporated and dispersed into the atmosphere (without burning).

Presented below are graphics showing the sea surface area covered by the LNG pool, the radiation contours if LNG is assumed to burn, and the concentrations of LNG in the atmosphere (10 m elevation) if the vapor disperses from the spill. The footprint of the LNG pool, the dispersed cloud and thermal radiation, and the incident energy flux are shown versus time for each case. Mass balances for each case are then provided showing the mass of LNG in the tank, on the sea surface, and either evaporated or burned versus time.

4.1. Area of LNG on sea surface, thermal radiation field, and dispersed

Fig. 7 shows the model predicted area of LNG on the water surface over the course of the simulation for the three cases. The graphics were created by overlaying multiple model results, at 4 min time intervals, during the simulations. They hence con-

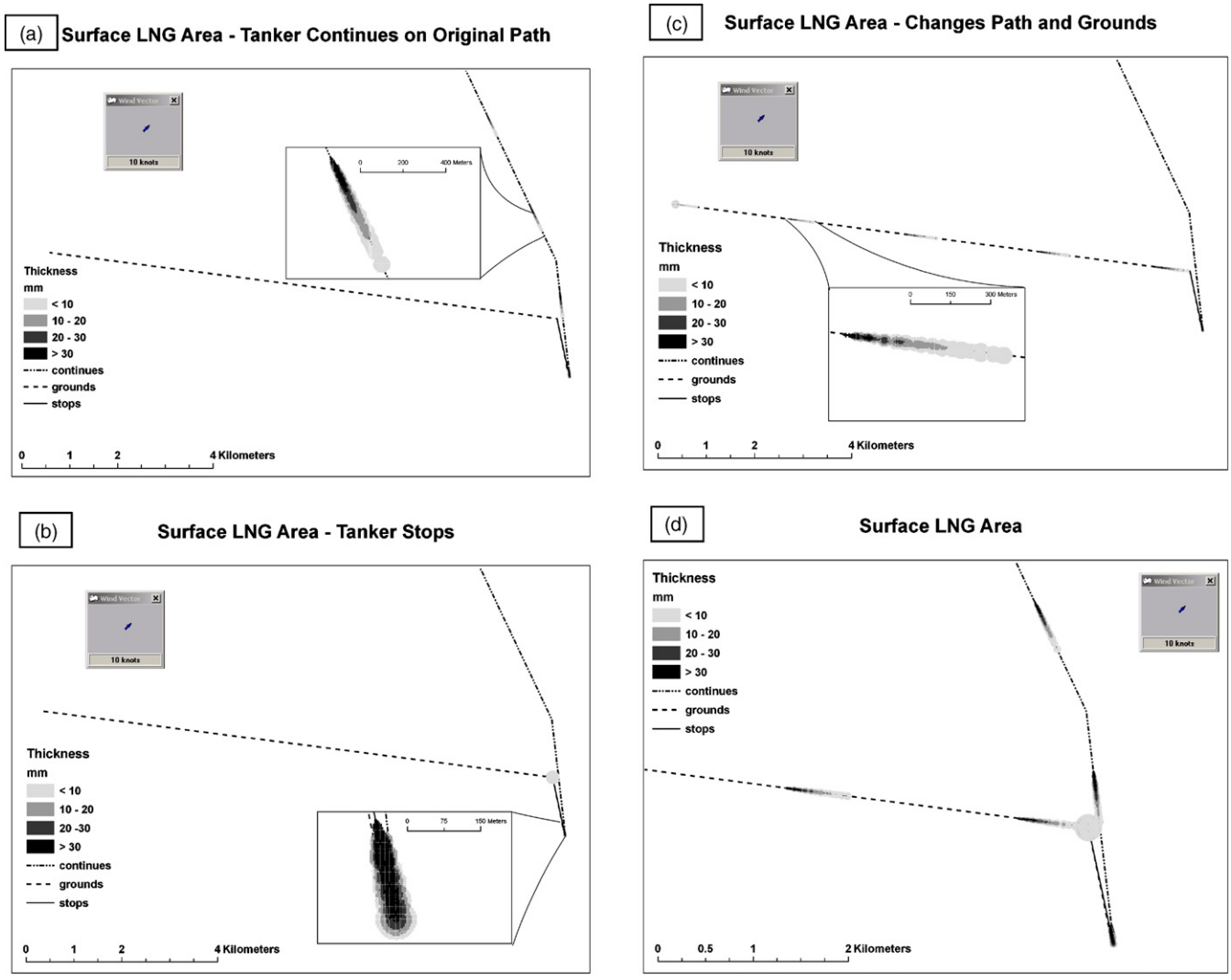

Fig. 7. LNG on the water surface area in 4-min intervals: (a) tanker continuing on course (Case 1), (b) tanker stopping (Case 2), (c) tanker grounding (Case 3), and (d) all cases combined. Thickness contours for each case are provided. The insert shows a close-up view at one time increment.

stitute snapshots as the release unfolds. An insert is provided for each case to allow visualization of the thickness contours. The last panel provides the results of all cases overlaid to facilitate comparisons. For both the moving cases (Cases 1 and 3), the LNG forms an elongated plume behind the vessel. The thickness of the LNG is greatest in the immediate vicinity of the moving source and decreases with distance behind the vessel. The plume width is controlled by the tank release and evaporation rates and the vessel speed. Both cases show a similarly sized area given the fact the vessel and wind speeds and the tank release rate are the same. If the vessel stops however the area is circular in shape and covers a much large area in the immediate vicinity of the stopping location.

Fig. 8 shows the model predicted thermal radiation contours (5–12, 12–25, 25–38, and greater than 38 kW/m^2) over the course of the simulation for the three cases. The last panel provides the results of all cases overlaid to facilitate comparisons. The results are shown at 3-min intervals over the time period of the release. For Case 1 the impacted area for a given thermal radiation contour decreases in size with time until eventually disappearing 35 min after the release begins. This behavior is a direct result of the declining release rate with time from the vessel. If the vessel stops (Case 2) the radiation field is restricted to the immediate vicinity of the vessel and of course impacts a larger area than for the moving cases. If the vessel is grounded (Case 3), the radiation field along the vessel track shows similar behavior to the continuing on course example (Case 1) while underway and reverts to the stopped case (Case 2) when the vessel eventually grounds. In the present simulation, the tanker is still releasing LNG when it grounds and hence a circular radiation field is seen at the end of the vessel track. A close inspection of the figures shows that if the vessel is in motion the radiation contours become elliptical, with the major axis oriented in the direction of vessel motion.

Fig. 9 shows the model predicted vapor cloud area and associated concentration contours (2.5–5, 5–15; and greater than 15%) over the course of the simulation for the three cases. The last panel provides the results of all cases overlaid to facilitate comparisons. The results are shown at 3-min time intervals over the period of the release. For all cases the vapor cloud is transported

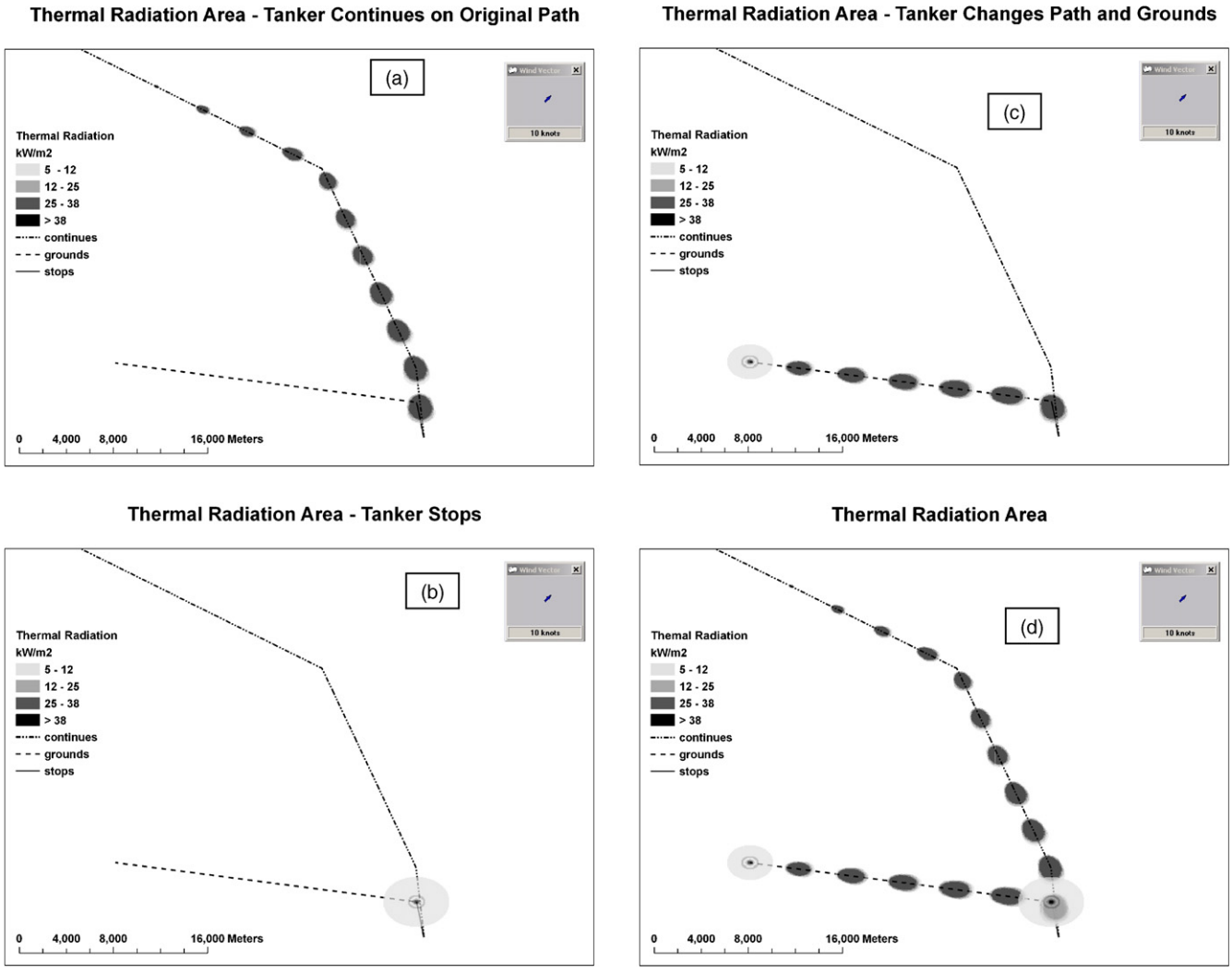

Fig. 8. Thermal radiation areas in 3-min intervals for the: (a) tanker continuing on course (Case 1), (b) tanker stopping (Case 2), (c) tanker grounding (Case 3), and (d) all cases combined. Contours are shown at 3 min intervals. Thermal radiation contours for each case are provided.

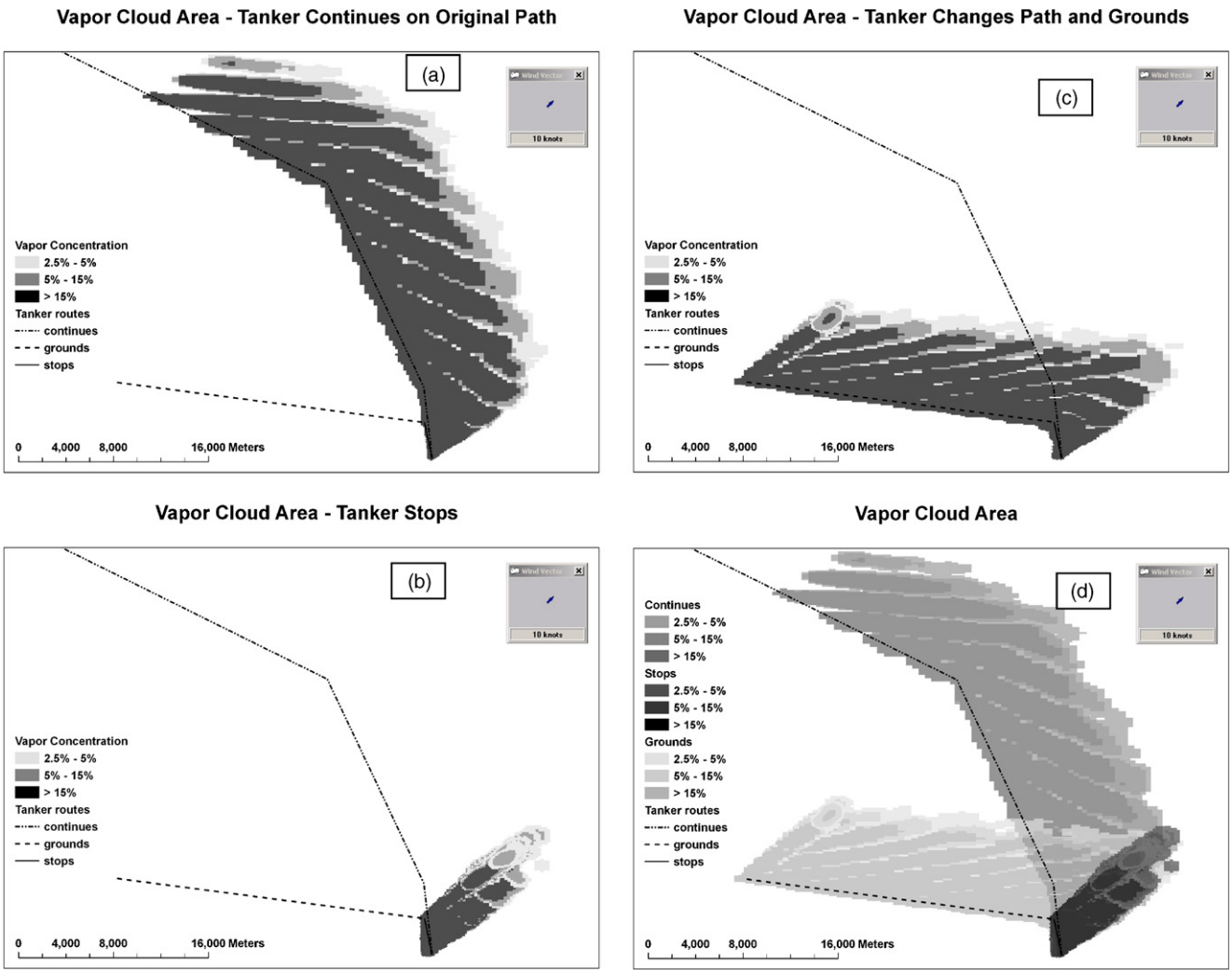

Fig. 9. Vapor cloud swept area in 3-min intervals for the: (a) tanker continuing on course (Case 1), (b) tanker stopping (Case 2), (c) tanker grounding (Case 3), and (d) all cases combined. Contours are shown at 3 min intervals. Vapor contours for each case are provided.

and dispersed down wind from the release location. The highest concentrations are in the core of the plume with lower concentrations at the margins, and particularly at the downwind end of the plume. The length of the plume is controlled by the release strength, the vertical dispersion coefficient, and degree of stability in the atmosphere. The vessel's forward speed and direction and the wind speed and direction establish the orientation of the vapor cloud to the vessel track. This is nicely illustrated in the on-course case (Case 1) by the change in the orientation of the vapor cloud when the vessel changes from a north–northwesterly to west–northwesterly direction. It is interesting to note that the vapor cloud retains a memory of the change in vessel course (compare orientation of the vapor plume near the vessel track and at the downwind end of the plume after the change of course has occurred). The last two vapor cloud snapshots are detached from the vessel track since the release has ceased and the cloud is being transported away from the vessel by the wind. It is also noted that the last release shown has lower concentrations in the core than its predecessors. This is due to the substantially reduced release rate from the tank near the end of the discharge. The swept area for the stopping case (Case 2) is essentially downwind given the vessel's initial northerly motion and then its fixed location at the stopping point. The plume length increases once the vessel stops. The grounding case (Case 3) has characteristics similar to the on-course case (Case 1) when the vessel is underway and of the stopping case (Case 2) once the vessel grounds.

Comparing the three cases, if the vessel continues to move either on course or to a grounding location, the LNG vapor concentrations are lower but distributed over a much wider area than if the vessel stops.

Figs. 10–12 show the LNG surface pool area and the area with thermal intensity greater than 5 kW/m^2, if the release burns, or the plume concentrations (greater than 5% and between 5 and 15%) if the vapor disperses from the spill, for Cases 1, 2, and 3, respectively. The release rate from the tank is shown for reference. Each case is discussed separately below. The pool areas for most of these cases are small compared to the thermal radiation and dispersed plume areas and impossible to read from the figures. They are therefore presented in Fig. 13 using an expanded scale.

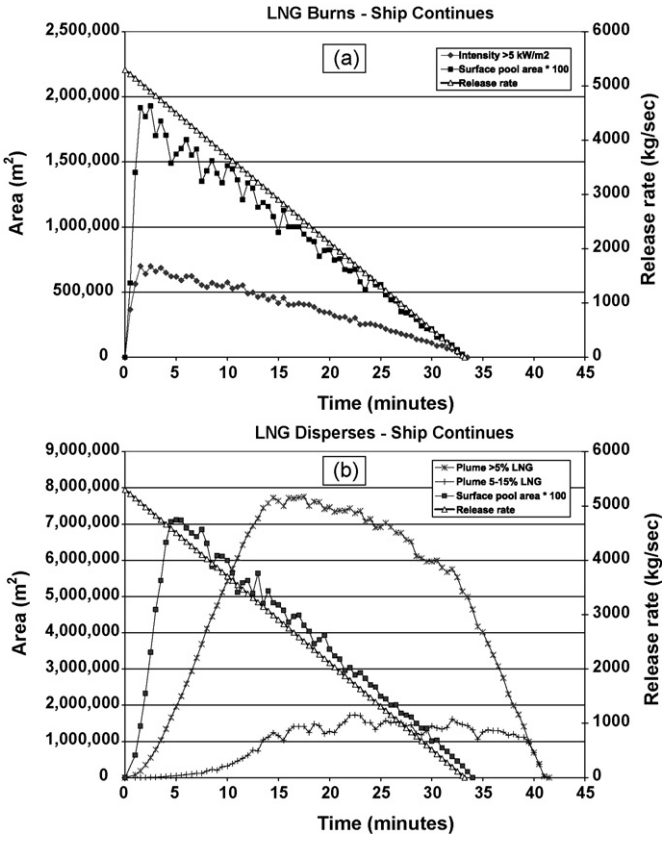

Fig. 10. Area of LNG surface pool, area with radiation intensity above 5 kW/m^2, and plan view area of vapor cloud with concentrations above 5% and between 5 and 15% as a function of time since the start of the release for the vessel continues case (Case 1). The upper panel (a) assumes burning and the lower panel (b) that the gas disperses into the atmosphere. The release rate from the vessel is provided for reference. The value for the pool area has been scaled by a factor of 100 to make it readable.

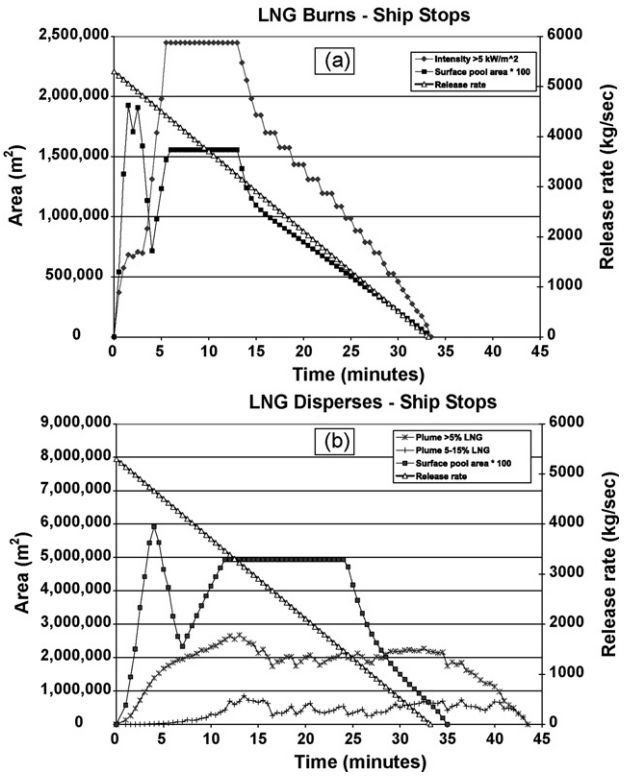

Fig. 11. Area of LNG surface pool, area with radiation intensity above 5 kW/m^2, and plan view area of vapor cloud with concentrations above 5% and between 5 and 15% as a function of time since the start of the release for the vessel stopping case (Case 2). The upper panel (a) assumes burning and the lower panel (b) that the gas disperses into the atmosphere. The release rate from the vessel is provided for reference. The value for the surface pool area has been scaled by a factor of 100 to make it readable.

4.2. Vessel continues (Case 1)

If the vessel remains on course and the LNG burns (Fig. 10a), the surface pool spreads on the water surface over the first 2 min. During this period the release rate exceeds the burning rate and the pool increases in size. When the release rate and burning rate are equal the pool reaches its peak size. The area, with radiation intensity above 5 kW/m^2, also reaches its peak value at this time. After this time, the release rate and burning rate are in balance and the radiation area declines gradually as the release rate decreases. The short term variations in the curves are a result of the particle based approach employed in the model and to the continuing aggregation of the gas spillets.

If burning does not occur (Fig. 10b), vapor begins to disperse into the atmosphere and is transported and dispersed by the surface winds. The dispersed vapor cloud (measured as concentrations, 10 m above the surface, greater than 5% or between 5 and 15%) grows rapidly until reaching its maximum size, approximately 15-min after the start of the simulation. The peak areas for the dispersed vapor cloud occur when the release rate from the surface pool is balanced by the dilution of the vapor plume in the atmosphere. At later times, the affected area decreases with time in response to the declining release rate. The tank is fully drained at 33.3 min but the vapor cloud remains at concentrations above 5% for an additional 10 min. During this period the surface pool of LNG no longer exists and hence does not act as a source for the dispersed gas. The vapor cloud is subject to dilution by atmospheric mixing near the sea surface and concentrations eventually decrease to levels below the LFL (5%). Because the underlying processes are the same, the slope of the concentrations versus time during the build up phase (3–15 min) and the disappearance phase (33–43 min) are almost of identical magnitude (with opposite sign). At its peak, the area with values above 5% is about five times larger than that with values between 5 and 15%. This is the result of mixing and clearly evident on the sides and down stream end of the vapor plumes. The regions on the downstream end of the plume have had the most time in the atmosphere and hence the most time to mix and dilute (Fig. 9).

4.3. Vessel stops (Case 2)

Fig. 11 shows the surface areas versus time for the vessel stopping case, for both the LNG burning (Fig. 11a) and LNG dispersing (Fig. 11b) scenarios. Three minutes after the release begins, the vessel comes to a full stop. During this initial period while the vessel is still underway, for the burning scenario both the area of the radiation intensity greater than 5% and the surface

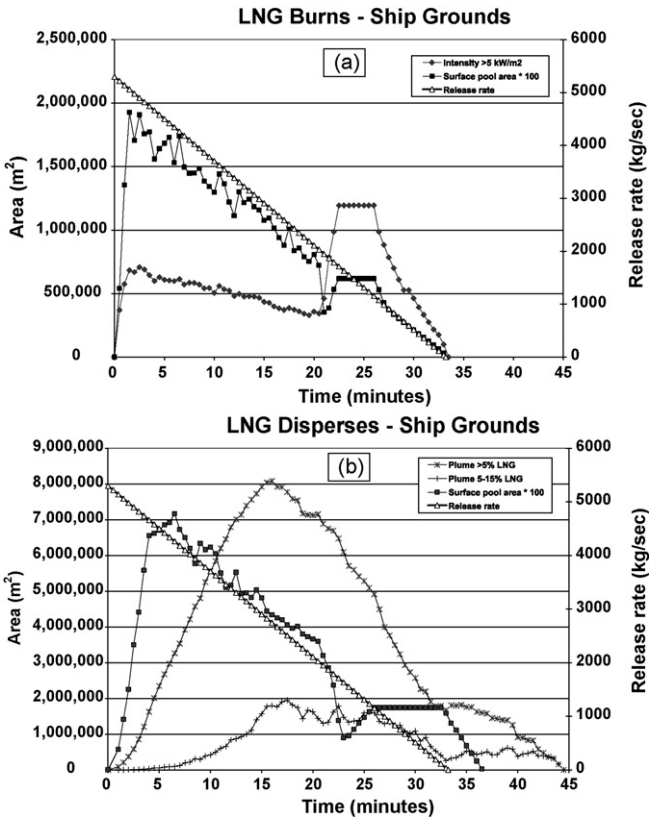

Fig. 12. Area of LNG surface pool, area with radiation intensity above 5 kW/m^2, and plan view area of vapor cloud with concentrations above 5% and between 5 and 15% as a function of time since the start of the release for the vessel grounding case (Case 3). The upper panel (a) assumes burning and the lower panel (b) that the gas disperses into the atmosphere. The release rate from the vessel is provided for reference. The value for the pool area has been scaled by a factor of 100 to make it readable.

pool reach a terminal size, as in Case 1 (Fig. 10a). Once the vessel stops however the surface pool rapidly increases in size since the release into the surface pool surrounding the vessel exceeds the burning rate. Six minutes after the start of the release, the radiated area reaches its maximum value, with the burn rate in balance with the release rate. This continues for an additional 7.5 min. From this time until the end of the release, the radiated area decreases as the release rate decreases. This response is exactly analogous to the validation case presented in Section 3. For the no burning scenario, the increase in area of the dispersed vapor cloud to equilibrium conditions followed by gradual decline with time is the same as for Case 1, but the peak values are much lower (factor of 4). Similar to Case 1, the cloud remains for 10 min after the release stops.

4.4. Vessel grounds (Case 3)

The results for the vessel grounding are shown in Fig. 12. For the burn scenario the results are exactly the same as in Case 1 for the first 22 min after the release, at which time the ship grounds. The behavior thereafter is the same as that for vessel stopping case (Case 2) with a rapid increase in the area of the radiated field, followed by a constant area phase, and eventually a decreasing area with time until the LNG disappears from the water surface. The peak thermally radiated area in the grounding case is less than half of that for the stopping case (Case 2). This of course reflects the loss of gas through burning while the vessel was still underway. For the no burning scenario, the first phase is identical to the vessel continues case (Case 1) and the later portion to the vessel stopping case (Case 3). As for the stopping case, the dispersed cloud persists for 12 min after the release has ceased.

Figs. 13–15 show the surface pool area, thermal radiation area, and the vapor cloud area (greater than 5%, and between 5 and 15%) versus time, respectively. The results for the three cases are overlaid to facilitate comparisons. The LNG pool on the water surface is shown in Fig. 13a and b for the scenarios with and without burning, respectively. The shapes of the curves *with* and *without* burning for the ship continues on-course case are exactly the same: a rapid rise to a peak value, followed by a long linear decline until the release ceases. The peak area impacted is approximately 3.5 times higher and 3 min later for the *without* than the *with* burning scenario. This is a reflection of the substantially increased mass transfer rate from the surface pool *with* burning. For the cases where the vessel stops, the pool area shortly after stopping increases to a peak value, remains at this level for some number of minutes and then asymptotically

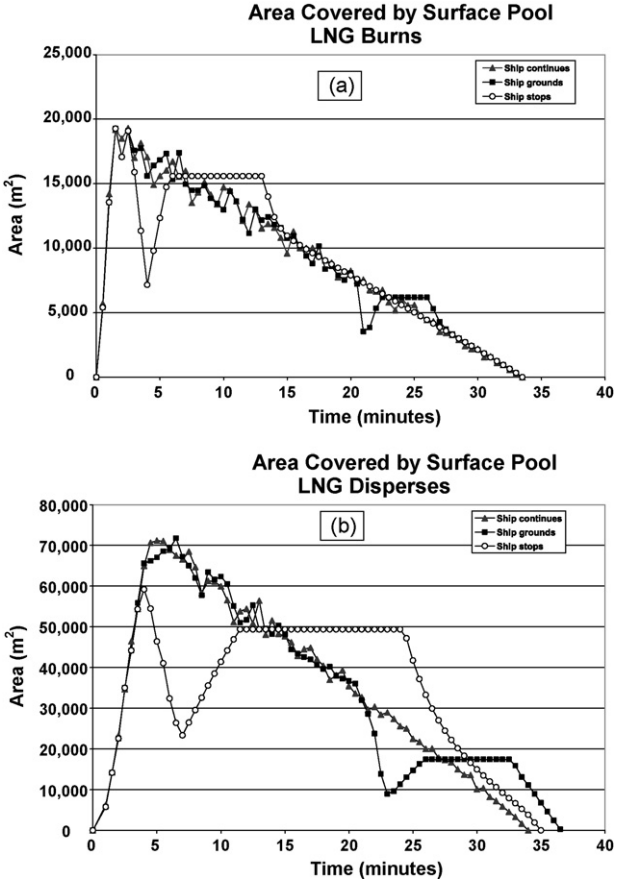

Fig. 13. Area of LNG surface pool a function of time since the start of the release for the vessel continuing (Case 1), stopping (Case 2), and grounding cases (Case 3), (a) with burning (upper panel) and (b) dispersing (lower panel).

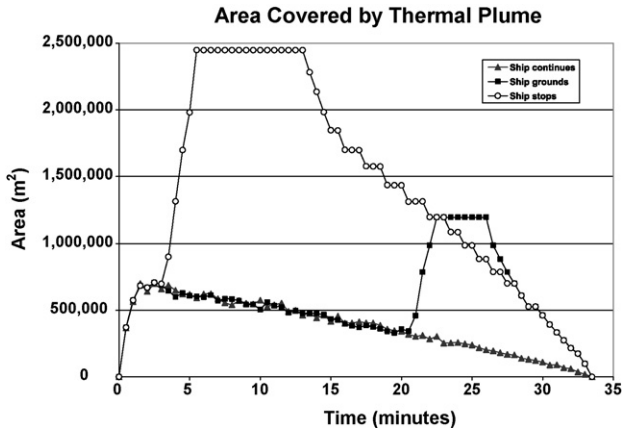

Fig. 14. Area with radiation intensity above 5 kW/m^{2}as a function of time since the start of the release for the vessel continuing (Case 1), stopping (Case 2), and grounding case (Case 3).

approaches the results for Case 1. It is seen that the earlier the time of stopping, the greater the release rate, the larger the pool maximum area, and the longer its duration. Pool areas are larger and the rise/fall rates are more rapid for the *without* burning case. The simulations show that the minimum pool area occurs when the vessel continues on course (Case 1).

Fig. 14 shows the area of radiated thermal plume versus time for the three release scenarios. The shapes of the curves are a direct reflection of the surface pool areas. The earlier the vessel stops the larger the impacted area and the longer it lasts. The minimum area is once again observed for the vessel continuing on-course case.

Fig. 15a and b present the time history of the dispersed vapor cloud area for the three release cases, for the greater than 5% contour and the 5–15% contour, respectively. In all cases the affected area rises to a peak value, after which it decreases. The rate and timing of the decrease depend on both the LNG surface pool area and the environmental conditions. The dispersed area is largest for the ship continuing on-course case (Case 1) and smallest for the vessel stopping case (Case 2).

A review of all three cases shows the following:

(1) The area of the surface pool versus time for all cases (both burn and dispersed scenarios) shows a growth to a maximum size in the first few minutes after the release followed by a long slow decline until the end of the simulation. The largest area achieved is based on a balance between the release rate and burning/evaporation rate. The time scale for this is determined by the spreading rate. The peak size for the dispersed case is about 3.5 times that for the burned case, reflecting the fact that burning has a higher rate of transfer

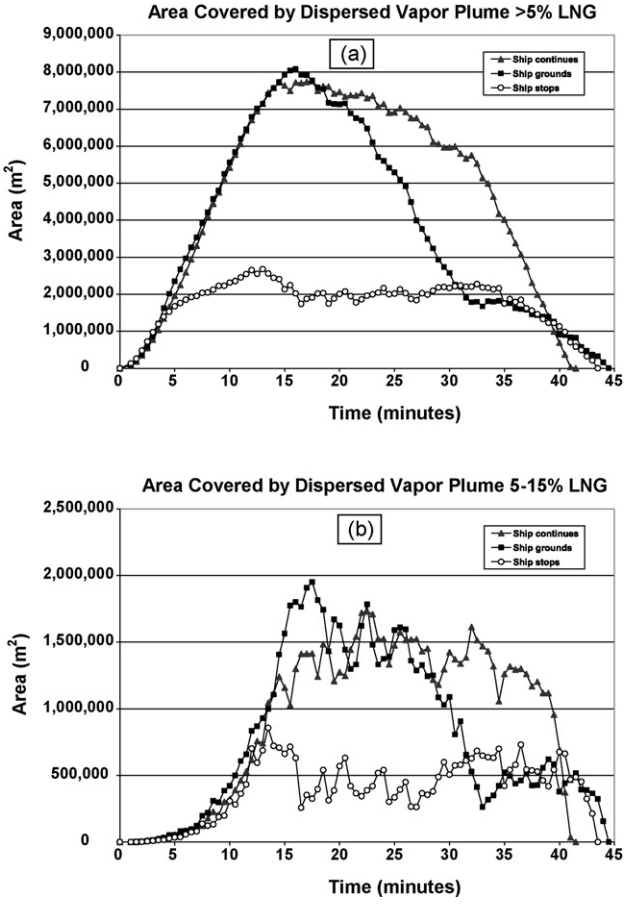

Fig. 15. Plan view area of vapor cloud with concentrations above 5% (a) and between 5 and 15% (b) a function of time since the start of the release for the vessel continuing (Case 1), stopping (Case 2), and grounding cases (Case 3).

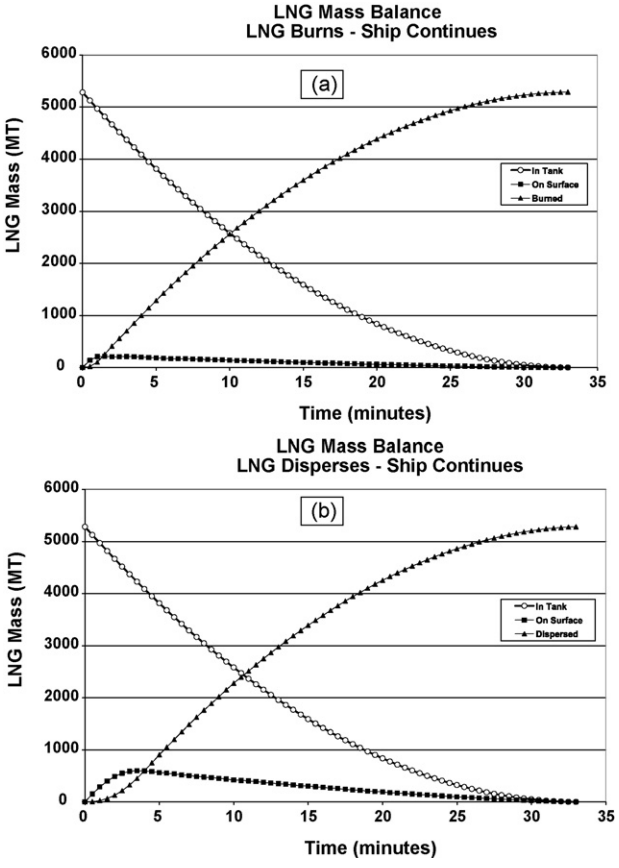

Fig. 16. LNG mass balance (in tank, on surface, and burned or dispersed) for ship continues on course (Case 1): (a) LNG burns and (b) disperses in form of vapor cloud.

of gas from the sea surface than normal evaporation. The decreasing pool size versus time, after this peak, reflects the decreasing source strength. This basic pattern is altered if the vessel stops, but only temporarily.

(2) The area of the radiated field (burning) is minimized if the vessel remains in motion and dramatically increases in size if the vessel stops. The later the vessel stops, the smaller the difference between the vessel moving and stopping cases. For the present simulation, the differences in areas are a factor of 5 between the moving and stopping after 5 min cases.

(3) The area of the dispersed vapor cloud (no burn case) increases to a peak value and then decreases to zero about 10 min after the end of the release. A balance between the release rate, the evaporation rate (which in turn is dependent on the pool size) and the atmospheric dispersal or mixing rate govern the time scale and peak value of the dispersed cloud area. In the initial stages, the release rate exceeds the evaporation rate and the pool size continues to grow, which subsequently results in an increase in the loss rate from evaporation. The vapor cloud continues to grow until the input rate is balanced by mixing. When these rates are equal the dispersed cloud area reaches its maximum value. It declines after this time as the release rate decreases, the pool size shrinks, and the evaporation rate declines. The area of the vapor cloud is minimized if the vessel stops and maximized if the vessel is moving.

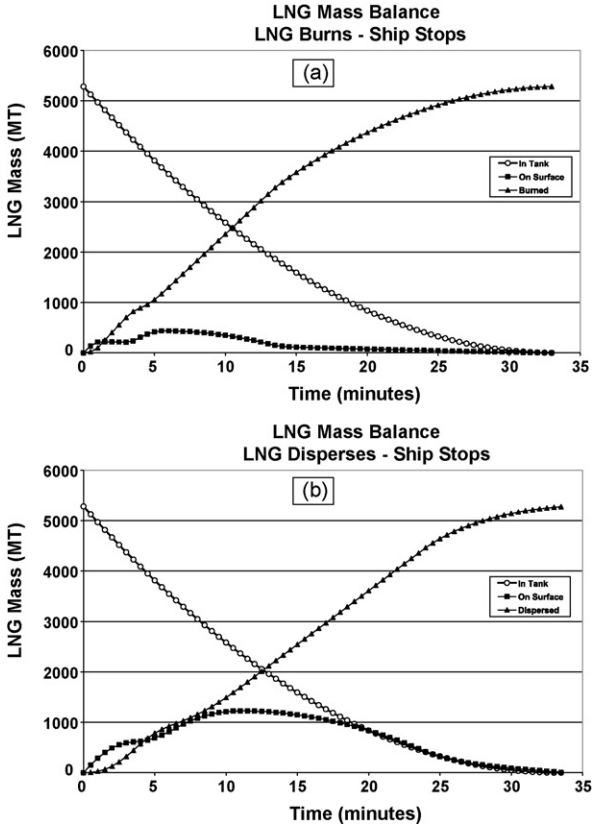

Fig. 17. LNG mass balance (in tank, on surface and burned or dispersed) for ship stops case (Case 2), (a) LNG burns and (b) disperses in form of vapor cloud.

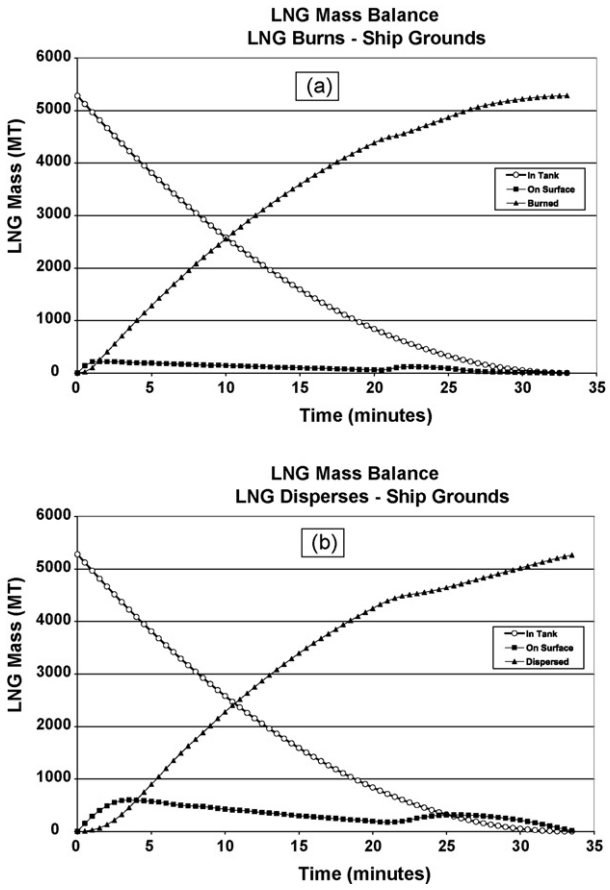

Fig. 18. LNG mass balance (in tank, on surface, and burned or dispersed) for ship grounds case (Case 3), (a) LNG burns and (b) disperses in form of vapor cloud.

4.5. Mass balances

The mass balances for the three cases are shown in Figs. 16–18 for both the burning (a) and evaporating (b) scenarios. For each case, the LNG mass in the tank, on the surface, and burned or evaporated versus time is provided. In all cases the release rate is exactly the same, with the maximum value at the beginning of the simulation and declining with time. This is a result of the head-based release rate from the tank. For Case 1 (vessel on course, Fig. 16) the mass on the surface reaches its maximum value after 1.5 and 3 min, respectively for burn and no burn scenarios. Surface mass declines gradually with time after this point. The predictions show that the LNG is rapidly removed from the surface (either by burning or evaporation) after it is released. The amount on the sea surface is larger for the evaporation than the burn scenario (see peak values) due to the lower mass loss rate from the surface pool.

For the vessel stopping case (Case 2) the mass balance versus time (Fig. 17) has a similar shape to the vessel continuing case (Case 1) until the vessel comes to a full stop (3 min). Once the vessel stops, the amount on the surface continues to increase reaching peak values 5 and 10 min after the start of the simulation for the burn and no burn cases, respectively. The amount on the surface continues to disappear until the tank is empty. The rapid

transfer from the sea surface to the atmosphere via burning or evaporation is once again noted.

The grounding case (Case 3) shown in Fig. 18 is a hybrid of the vessel continuing and grounding cases. The transition between the two occurs after the vessel has grounded, about 20 min after the start of the simulation.

5. Conclusions

A model to predict the transport and fate of marine spills of LNG has been developed within a geographic information system framework. A particle based approach was implemented, with algorithms to predict a time dependent release rate from a tank with a user defined breach size, spreading of the LNG on the sea surface, advection of the pool due to surface currents and waves, evaporation from the pool to the atmosphere (with or without burning), and radiated incident energy flux, if the LNG ignites, or characteristics of the dispersed vapor cloud, if it does not. The model allows for releases from both stationary and moving point sources. The latter can be specified by a user defined vessel track.

The model was validated against prior time dependent release simulations performed by ABS Consulting [2] (with and without burning) and steady state simulations provided in Sandia [1] (with burning). Model predictions were in excellent agreement with the ABS Consulting results. Comparisons with the Sandia predictions were reasonable, given the differences in the model assumptions and formulations.

To illustrate the model predictive capability for realistic emergency response scenarios, simulations were performed for a tanker entering Block Island Sound. Three cases were studied, the first assuming that the vessel continues on course after the spill starts, the second assuming that the vessel stops as soon as practical after the release begins (3 min), and the third assuming the vessel grounds at the closest site practical.

In applying the model to these cases the following observations were made:

1. Given the very short time scales for the releases (minutes) and slowly varying ocean current and atmospheric conditions over these time scales, assuming that the currents and winds are constant over the length of the simulation is a reasonable first approximation. It is noted that observation and model forecasting systems typically provide data on hourly to several hourly intervals.
2. Ocean currents typically have speeds in the range of 0.1 to several m/s. For the present application the maximum tidal currents are 50 cm/s and hence can result in maximum displacements on the order to 0.9 km over the duration of a 30 min release. This distance is larger than the maximum size of the pool radius and hence current transport plays an important role in the spill's evolution.
3. The areas of the surface pool and the incident thermal radiation field (with burning) are minimized and the dispersed vapor cloud area (without burning) is maximized if the vessel continues on course. The surface pool area for the case with burning is substantially smaller than for the without burning case because of the higher mass loss rate from the surface slick due to burning. With the vessel on course, the speed of the vessel movement substantially exceeds the spill spreading rate and hence both the thermal radiation fields and surface pool trail the vessel. The relative directions and speeds of the wind and vessel movement govern the movement of the dispersed plume.

   If the vessel stops, the areas of the surface pool and incident radiation field (with burning) are maximized and the dispersed cloud area (without burning) is minimized. The longer the delay in stopping the vessel, the smaller the peak values are for the pool area and the size of the thermal radiation field. Once the vessel stops the spill pool is adjacent to the vessel and moving down current. The thermal radiation field is oriented similarly. The optimal configuration is for the vessel to be oriented into the currents so that the surface pool is in the wake of the vessel.

   The model results have important implications in vessel response during a spill event where the relative benefits of keeping the ship moving must be balanced against the larger swept area of the vapor cloud and/or radiation field. Contingency planning along the ship track may result in different response strategies depending on location. The addition of real time or forecasted meteorological and oceanographic information provided directly to the ship's command center may be important in determining the appropriate response to minimize the hazard.

Given LNGMAP's modular, algorithm based designed it is ideally suited to incorporate new algorithms as they became available and can readily be used to perform sensitivity analyses. The global re-locatability of the system and ability to link to world wide oceanographic and meteorological models facilitate application to any location.

The atmospheric dispersion model, while functional and providing reasonable estimates of the dispersion of the vapor cloud, is at best an *ad hoc* solution. It has the benefit of being integrated into LNGMAP and directly linked to the evaporative losses from the surface pool. It is reasonable for first level screening analyses but should be replaced by a more sophisticated dense gas model (see Touma et al. [21] for a review of the performance of these models) for more detailed analyses.

The flame model should be refined to include the effects of incomplete combustion due to oxygen starvation and radiative shielding by soot by the use of appropriate algorithms, ideally developed from full CFD flame modeling, as suggested by Sandia [1]. The particle-based approach used in LNGMAP, with discretely burning pools or flamelets, is well suited to this refinement.

At this stage of development LNGMAP is suitable for discrete simulations of a variety of spill scenarios. These scenarios can include variations in breach size, tank volume and configurations, environmental forcing (winds and currents), and movement of the vessel. Extensions of the approach to include stochastic simulations where the above variables can be changed over a suitable statistical range are straightforward but remain to be performed.

The present release model provides reasonable estimates for the simple breach shape but should be extended to account for more complicated hole shapes [22], breaches above and below the water line [3], and the effects of partial vacuum in un-vented tanks (glug–glug effects). Improvements in the behavior of LNG when it mixes with sea water including heat transfer and dissolution are recommended, as are inclusion of time varying physical and chemical properties based on temperature and fraction evaporated.

LNGMAP is designed to be a planning tool that provides more realistic spill consequences than the simple, static approaches found in the ABS Consulting [2] but yet is a much more efficient PC-based calculation than a full CFD approach.

References

[1] Sandia National Laboratories, 2004. Guidance on Risk Analysis and Safety Implications of a Large Liquefied Natural Gas (LNG) Spill Over Water. Sandia Report SAND2004-6258. December 2004.

[2] ABS Consulting Inc., 2004. Consequence assessment methods for incidents involving releases from liquefied natural gas carriers, Report prepared for Federal Energy Regulatory Commission, contract FERC04C40196. May 13, 2004.

[3] J. Fay, Model of spills and fires from LNG and oil tankers, J. Hazard. Mater. B96 (2003) 171–188.

[4] W. Lehr, D. Simecek-Beatty, Comparison of hypothetical LNG and fuel fires on water, J. Hazard. Mater. 107 (2004) 3–9.

[5] Quest, Modeling LNG Spills in Boston Harbor, Quest Consultants, Inc., 2001, 2003.

[6] Vallejo, 2003. LNG Health and Safety Committee of the Disaster Council City of Vallejo, CA, LNG in Vallejo: Health and safety issues, January 26, 2003.

[7] Applied Science Associates, Inc. (ASA), OILMAP Technical Manual, Applied Science Associates, Inc., Narragansett, RI, 2005.

[8] Applied Science Associates, Inc., (ASA), CHEMAP Technical Manual, Applied Science Associates, Inc., Narragansett, RI, 2006.

[9] FERC, 2004. Notice of availability of staff's responses to comments on the consequence assessment methods for incidents involving releases from liquefied natural gas carriers, Federal Energy Regulatory Commission, Docket No. AD04-6-000, June 18, 2004.

[10] G.T. Csanady, Turbulent Diffusion in the Environment, D. Reidel Publishing Company, Boston, MA, 1976.

[11] Webber, D.M., 1990. Model for pool spreading and vaporisation and its implementation in the computer code GASP, SRD/HSE-report R507, September 1990.

[12] TNO, in: C.J.H. van den Bosch, R.A.P.M. Weterings (Eds.), Methods for the Calculation of Physical Effects, 'Yellow Book", CPR 14E, 3rd ed., The Hague, The Netherlands, 2005, Second revised print.

[13] V.V. Kilmenko, Film boiling on a horizontal plate—new correlation, Int. J. Heat Mass Transfer 24 (1981) 69–79.

[14] NOAA (National Oceanic and Atmospheric Administration), ALOHA™ (Areal Locations of Hazardous Atmospheres) 5.0 Theoretical Description, NOAA Technical Memorandum NOS ORCA 65, Seattle, WA, 1992.

[15] G.A. Briggs, Diffusion Estimation for Small Emissions. ATDL Contribution File No. 79, Atmospheric Turbulence and Diffusion Laboratory, 1973, p. 85.

[16] J. Havens, T. Spicer, 1985. Development of an atmospheric dispersion model for heavier-than-air gas mixtures, vol. I. Report CG-D-22-85. U.S. Coast Guard.

[17] P.H. Thomas, The size of flames from natural fires, in: Proceedings of the Ninth International Symposium on Combustion, Combustion Institute, Pittsburgh, PA, 1962, pp. 844–859.

[18] P.J. Rew, W.G. Hulbert, Development of pool fire thermal radiation model, HSE Contract Research Report No. 96-1996, Health and Safety Executive, 1996.

[19] K.S. Mudan, Thermal radiation hazards from hydrocarbon pool fires, Progr. Energy Combust. Sci. 10 (1984) 59–80.

[20] M. Ward, M. Spaulding, A nowcast/forecast system of circulation 'dynamics in Narragansett Bay, in: Proceedings of Seventh International Conference on Estuarine and Coastal Modeling, sponsored by the University of Rhode Island Conference Office, St. Peter, Florida, November 5–7, 2001, 2002, pp. 1002–1022.

[21] J.S.A. Touma, W.M. Cox, H. Thistle, J.G. Zapert, Performance of dense gas dispersion models, J. Appl. Meteorol. 54 (1995) 603–615.

[22] F.T. Dodge, E.B. Bowles, J.E. Mann, R.E. White, Experimental Verification and Revision of the Venting Rate Model of the Hazardous Assessment Computer System and the Vulnerability Model, US Coast Guard, Research and Development Center, Groton, CT, 1980.